

Integrated Wind Farm Design: Optimizing Turbine Placement and Cable Routing with Wake Effects

Jaap Pedersen^{i,a}, Niels Lindner^{ii,a}, Daniel Rehfeldt^{iii,a}, and Thorsten Koch^{iv,a,b}


^aZuse Institute Berlin, Berlin, Germany


^bTechnische Universität Berlin, Berlin, Germany


Abstract

An accelerated deployment of renewable energy sources is crucial for a successful transformation of the current energy system, with wind energy playing a key role in this transition. This study addresses the integrated wind farm layout and cable routing problem, a challenging nonlinear optimization problem. We model this problem as an extended version of the Quota Steiner Tree Problem (QSTP), optimizing turbine placement and network connectivity simultaneously to meet specified expansion targets. Our proposed approach accounts for the wake effect – a region of reduced wind speed induced by each installed turbine – and enforces minimum spacing between turbines. We introduce an exact solution framework in terms of the novel Quota Steiner Tree Problem with interference (QSTPI). By leveraging an interference-based splitting strategy, we develop an advanced solver capable of tackling large-scale problem instances. The presented approach outperforms generic state-of-the-art mixed integer programming solvers on our dataset by up to two orders of magnitude. Moreover, we demonstrate that our integrated method significantly reduces the costs in contrast to a sequential approach. Thus, we provide a planning tool that enhances existing planning methodologies for supporting a faster and cost-efficient expansion of wind energy.

ⁱ  0000-0003-4047-0042, corresponding author, pedersen@zib.de

ⁱⁱ  0000-0002-8337-4387

ⁱⁱⁱ  0000-0002-2877-074X

^{iv}  0000-0002-1967-0077

Keywords

OR in energy, combinatorial optimization, quota Steiner tree problem, wind farm design, wake effect

1 Introduction

The transformation of the existing energy system including an increasing deployment of renewable energy sources is vital to reduce global greenhouse gas emissions and to mitigate the impacts of climate change. Wind energy has proven to be an established source of electricity in this transformation (Veers et al., 2019). The global wind capacity has increased by more than 20% annually between 2000 and 2019 (Pryor et al., 2020), reaching 730 GW in 2020 (Our World in Data, 2021), with a further increase of 50% expected by the end of 2023 (Pryor et al., 2020). Additionally, a sharp decline of the already low cost of wind energy is expected by 2050 (Jansen et al., 2020; Wiser et al., 2016, 2021). This move towards renewable energy sources has created a more competitive market for companies investing in such technologies, making tools for designing and operating such systems optimally vital. With its impressive progress made in the last 20 years (Koch et al., 2022), mathematical programming has proven to be an efficient approach to tackle these challenging problems.

In this paper, we focus on the optimal design of wind farms. We present a novel approach for solving the *integrated wind farm layout and cable routing optimization problem* (IWFLCR). To this end, we introduce the *Quota Steiner tree problem with interference* (QSTPI). The QSTPI is an extension of the Steiner tree problem in graphs, and is enriched with important technical constraints such as maintaining a minimum distance between turbines and including wake effects. We formulate QSTPI as mathematical program in several ways, both as binary quadratic integer program, and as integer linear program. Furthermore, we propose a method to split QSTPI instances in two, exploiting information on lower bounds on the total interference, and thereby accelerating the solution process. Our methods are incorporated into the SCIP-JACK framework, a state-of-the-art branch-and-cut-based solver specialized for Steiner tree problems, moreover advancing its shortest path primal heuristic to handle wake effects. We demonstrate on a realistic benchmark set that our splitting strategy solves more

QSTPI instances, and about two orders of magnitude faster, than a black-box approach using the commercial solver GUROBI. Finally, we underline that there is a significant price of sequentiality, i.e., there are noteworthy quantitative benefits that can be obtained by solving the wind farm layout and cable routing optimization simultaneously instead of sequentially.

This paper is structured as follows. We begin with a literature review in Section 2. The QSTPI and its integer programming formulations are presented in Section 3. We propose a solution strategy based on splitting the total interference experienced in the wind farm in Section 4. We integrate our proposed model into SCIP-JACK and apply our new methodology in Section 5 on a large dataset. We highlight the benefits of using an integrated approach in contrast to the sequential one in Section 6. Finally, we discuss and conclude our method and results in Section 7.

2 Literature review

We will first review literature on wind farm planning in Section 2.1, and then proceed in Section 2.2 with our mathematical background, the Steiner tree problem.

2.1 Literature on wind farm planning

Designing wind farms involves a variety of decisions leading to many challenging optimization problems. In this paper, we focus on the integration of two main design tasks: the wind farm layout optimization (WFLO) and the wind farm cable routing (WFCR). There exists a vast amount of literature investigating both the WFLO and the WFCR. For an extensive overview we refer the reader to the surveys by Samorani (2013), Hou et al. (2019), and Fischetti and Pisinger (2019).

The WFLO maximizes the energy output of the wind farm. It does not only consider the number of turbines to be installed, but also takes the *wake effect* into account. A region of slower wind speed, a *wake*, is caused by each installed turbine, resulting in a reduced energy yield of turbines downwind. An investigation of the offshore wind farm areas along the US east coast by Pryor et al. (2021) shows that power reduction can be reduced by one-third due to wakes caused by upwind turbines and wind farms. Therefore, it is inevitable to consider the wake effect when modeling

the WFLO. There exists a variety of studies modeling the WFLO as a mixed integer programming problem (MIP). A first MIP is presented in Donovan (2005) based on the independent set problem. Turner et al. (2014) approximate the nonlinear optimization problem of minimizing the wake effect by a quadratic integer and a mixed integer linear programming model (MILP). Based on the MILP proposed by Archer et al. (2011), Fischetti and Monaci (2016) combine the MIP approach with a proximity search heuristic to solve large-scale instances with the drawback of losing proven global optimality.

In the WFCR, the costs of connecting the chosen turbines to the power grid are minimized. In the case of offshore wind farms, González et al. (2014) point out that the costs of the electrical infrastructure account for 15% to 30% of the overall initial costs of the wind farm, making them an essential matter of expenses. During the operation, power losses play a crucial role in terms of expected revenue. For example, Fischetti and Pisinger (2018) present a combination of MILP formulation and metaheuristics, named *matheuristics*, to minimize not only the initial costs, but also the reduced revenue due to power losses in the lifetime of a wind farm by considering cable capacities.

Due to the complexity of the WFLO and WFCR, the problems are usually solved sequentially. However, by design these problems are conflicting, i.e., WFLO aims to spread the turbines as far as possible to reduce wakes, whereas the WFCR tries to keep them as close as possible to reduce cable costs. Recent promising studies have been conducted to integrate these two problems balancing these conflicts (Cazzaro et al., 2023; Fischetti, 2021; Fischetti & Fischetti, 2022). Fischetti and Fischetti (2022) model the integrated layout and cable routing problem as a mixed-integer linear program in the context of offshore wind farms. The authors introduce a novel set of cutting planes and present combinatorial separation procedures integrated in a branch-and-cut solver. Although the problem is solved exactly, the approach is only performed on small instances with up to 40 potential turbine positions, whereas in practice, large wind farms might include up to 100 - 200 turbines¹. Recently, Cazzaro et al. (2023) approach the integrated layout and cable optimization problem heuristically using an adapted variable neighborhood search. Even though the heuristic combining layout and cable routing provides better solutions than the previously proposed sequential

¹https://en.wikipedia.org/wiki/List_of_offshore_wind_farms; Retrieved on 2025/01/08

approach, it cannot provide any conclusion in terms of quality with respect to a globally optimal solution.

2.2 Literature, Algorithms and Software for Steiner Trees

The goal of this study is to provide a novel approach for solving the IWFLCR considering wake effects, minimum distance between turbines, and balancing investment cost and revenues. Conceptually, the IWFLCR is a network design problem with a number of additional constraints giving rise to a tree-shaped topology (Fischetti & Pisinger, 2018): We model the IWFLCR as an extension to the Steiner tree problem in graphs (STP), a classical NP-hard combinatorial problem (Karp, 1972), and one of the most studied problems in combinatorial optimization. Given an undirected graph with non-negative edge costs, the STP aims to find a tree that interconnects a given set of special points, referred to as *terminals*, at minimum cost. The STP and its variations arise in many real-world applications like, e.g., network design problems in telecommunication, electricity, or in district heating, as well as other fields such as biology; see, e.g., Leitner et al. (2014), Bolukbasi and Kocaman (2018), Ljubić et al. (2006), and Klimm et al. (2020), respectively. For a comprehensive overview of the STP and its variant the readers are referred to a recent surveys by Ljubić (2021), Rehfeldt (2021), and Pedersen and Ljubić (2025), and the references therein. In the PhD thesis by Ridremont (2019), the STP is applied to find a robust cable network for the purpose of designing a wind farm. Recently, Pedersen et al. (2024) have investigated the quota-constrained variant of the STP (QSTP) in the context of large-scale onshore wind farm planning. However, vital technical details, such as, among others, the wake effect or the minimum distance between turbines, are only implicitly modeled in the input data rather than in the optimization model. The authors introduce a novel transformation of the QSTP, which is integrated into the specialized Steiner tree solver SCIP-JACK, vastly outperforming state-of-the-art general out-of-the-box solvers. As an extension of the non-commercial general MIP solver SCIP (Bestuzheva et al., 2023), SCIP-JACK uses a branch-and-cut procedure to handle the exponential number of constraints induced by the Steiner cut-like constraints. These constraints will be recalled in Section 3.2. By additionally using various problem-specific reduction techniques and heuristics, SCIP-JACK has proven that it efficiently solves STP-related

problems of magnitudes larger than what general out-of-the-box MIP solvers can even load into memory; see, e.g., Rehfeldt and Koch (2022, 2023) and Rehfeldt et al. (2019). For a comprehensive description of SCIP-JACK’s operational principle the reader is referred to the PhD thesis by Rehfeldt (2021).

3 The Quota Steiner tree problem

We model the integrated wind farm layout and cable routing problem as a *Quota Steiner tree problem with interference* (QSTPI), extending and reformulating the classical quota Steiner tree problem (Johnson et al., 2000). In particular, we consider arbitrary tree-shaped network topologies. We introduce the QSTPI formally in Section 3.1, present a preliminary integer programming (IP) formulation in terms of directed cuts in Section 3.2, before applying the techniques by Pedersen et al., 2024 to obtain our final IP model in Section 3.3.

3.1 The Quota Steiner tree problem with interference

We adapt the formulation by Johnson et al. (2000) of the prize-collecting quota Steiner tree problem by adding vertex costs and integrating interference effects into the profit. Let $G = (V, E)$ be an undirected graph, whose vertex set V is partitioned into a set of *fixed terminals* T_f , a set of *potential terminals* T_p , and a set of additional *Steiner nodes*. We associate the potential terminals with *vertex costs* $b : T_p \rightarrow \mathbb{R}_{>0}$ and *quota profits* $q : T_p \rightarrow \mathbb{R}_{>0}$, referring to a *quota* $Q \in \mathbb{R}_{>0}$. Moreover, *edge costs* $c : E \rightarrow \mathbb{R}_{\geq 0}$ are given.

In terms of wind farm planning, the substations of the grid constitute T_f , while T_p represents the available wind turbine positions. The Steiner nodes allow for a more flexible cable routing. The vertex costs b and quota profits q model, e.g., the investment costs for a turbine and the turbine’s annual energy yield, respectively. The built turbines should contribute an output of at least the quota Q . The set of edges E represents the cable connections we can choose from, and c comprises their costs.

Each potential terminal, if chosen, may interfere with other potential terminals, reducing their assigned quota profit. As to wind turbine placement, each built turbine introduces a *wake*, an area of slower wind speed downstream, decreasing the power

production of the following turbines. We pin down this *wake effect* in a twofold way by *interference* and *minimum distance* notions: Let $I_{ij} \in \mathbb{R}_{\geq 0}$ be the interference experienced by the potential terminal $j \in T_p$ if the potential terminal $i \in T_p$ is chosen. Furthermore, let $d_{ij} \in \mathbb{R}_{\geq 0}$ denote the *distance* between two potential terminals $i, j \in T_p$, and let D_{\min} be a *minimum distance*.

Definition 3.1 (Quota Steiner Tree Problem with Interference). *Given an instance $(G, T_f, T_p, b, q, c, I, Q, d, D_{\min})$ with $G = (V, E)$ as above, the Quota Steiner Tree Problem with Interference (QSTPI) is to find a tree $S = (V', E') \subseteq G$ that contains all fixed terminals T_f , minimizes the total cable and turbine costs*

$$C(S) := \sum_{(i,j) \in E'} c_{ij} + \sum_{i \in T_p \cap V'} b_i, \quad (1)$$

fulfills the quota taking the induced interference into account:

$$Q(S) := \sum_{i \in T_p \cap V'} \left(q_i - \sum_{j \in T_p \cap V' \setminus \{i\}} I_{ji} \right) \geq Q, \quad (2)$$

and guarantees that $d_{ij} \geq D_{\min}$ for all $i, j \in V' \cap T_p$ with $i \neq j$.

3.2 Directed cut formulation

To develop an integer programming (IP) formulation, we transform the QSTPI into a variant of the *Steiner arborescence problem* (SAP). The general SAP is presented, e.g., in Wong (1984). The original undirected graph G is transformed into a directed graph $D = (V, A)$ where $A := \{(i, j), (j, i) : \{i, j\} \in E\}$. By shifting the costs of a vertex v onto the costs of its incoming arcs (see Ljubić et al., 2006), the arc costs are defined as

$$c(i, j) := \begin{cases} c_e + b_j & \text{if } j \in T_p, \\ c_e & \text{otherwise,} \end{cases} \quad \forall a = (i, j) \in A, \quad (3)$$

where c_e represents the cost of the corresponding edge $e = \{i, j\}$ in the original undirected graph G . For a subset of vertices $W \subseteq V$, we denote $\delta^+(W) := \{(i, j) \in A : i \in W, j \in V \setminus W\}$ as the set of outgoing arcs and $\delta^-(W) := \{(i, j) \in A : i \in V \setminus W, j \in W\}$ as the set of incoming arcs. For a single vertex i , we write $\delta^+(i) := \delta^+(\{i\})$ and $\delta^-(i) :=$

$\delta^-(\{i\})$. For any set K and any function $x : K \rightarrow \mathbb{R}$, we define $x(K) := \sum_{i \in K} x_i$.

We introduce a binary variable x_{ij} for each $(i, j) \in A$ if the arc (i, j) is contained in the Steiner tree ($x_{ij} = 1$) or not ($x_{ij} = 0$). Furthermore, let y_k be a binary variable for each $k \in T_p$ indicating whether or not the potential terminal k is chosen. The rooted directed cut IP formulation of the QSTPI with an arbitrary root $r \in T_f$ is given as follows:

$$\min \quad c^T x \tag{4}$$

$$\text{s.t.} \quad x(\delta^-(W)) \geq 1 \quad \forall W \subset V, r \notin W, |W \cap T_f| \geq 1 \tag{5}$$

$$x(\delta^-(W)) \geq y_i \quad \forall W \subset V, r \notin W, |W \cap T_p| \geq 1, i \in T_p \tag{6}$$

$$\sum_{i \in T_p} \left(q_i - \sum_{j \in T_p} I_{ji} y_j \right) y_i \geq Q \tag{7}$$

$$y_i + y_j \leq 1 \quad \forall i, j \in T_p, i \neq j, d_{ij} < D_{\min} \tag{8}$$

$$x_{ij}, y_k \in \{0, 1\} \quad \forall (i, j) \in A, \forall k \in T_p \tag{9}$$

The Steiner cut constraint (5) requires that any subset of nodes of the graph $W \subset V$ that does not contain the root ($r \notin W$), but at least one fixed terminal, i.e., $|W \cap T_f| \geq 1$, has at least one incoming arc. This guarantees that there exists a path from the root r to each $t \in T_f$. The same holds for (6), i.e., a path exists from r to the potential terminal $i \in T_p$ if it is chosen to contribute to the quota constraint (7) ($y_i = 1$). Finally, (8) ensures that no two potential terminals are chosen that are too close to each other.

3.3 Transformation

Having modeled the QSTPI as an IP by means of the directed cut formulation, we now shortly revisit the transformation of QSTP presented in Pedersen et al. (2024), which we extend by interference and minimal distance constraints. For each potential terminal $i \in T_p$, we add a new fixed terminal $i' \in T_f$. For each of these new fixed terminals i' , we create an arc (r, i') with costs $c(r, i') := 0$ and an arc (i, i') with costs $c(i, i') := 0$; see Fig. 1. Since i' is a fixed terminal, the Steiner cut constraint (11) then requires that $x_{i,i'} = 1$ or $x_{r,i'} = 1$. We interpret the first case as turbine $i \in T_p$ being built, and the latter case as turbine i not being built. Following the argumentation in Pedersen et al. (2024), instead of counting the collected quota, we limit the amount of

quota we can *waste*. Quota is wasted when a turbine i is not built, so that $x_{r,i'} = 1$, see (12). The total interference I_{tot} is given by the interference between all chosen turbines, see (13). The minimum distance constraint (14) prevents building simultaneously two turbines that are too close. The transformed QSTP including interference and minimum distance constraint is given as follows:

$$\text{QSTPI: } \min c^T x \quad (10)$$

$$\text{s.t. } x(\delta^-(W)) \geq 1 \quad \forall W \subset V, r \notin W, |W \cap T_f| \geq 1 \quad (11)$$

$$\sum_{i \in T_p} q_i x_{r,i'} + I_{\text{tot}} \leq \sum_{i \in T_p} q_i - Q \quad (12)$$

$$I_{\text{tot}} \geq \sum_{i \in T_p} \sum_{j \neq i \in T_p} I_{ij} x_{i,i'} x_{j,j'} \quad (13)$$

$$x_{i,i'} + x_{j,j'} \leq 1 \quad \forall i, j \in T_p, i \neq j, d_{ij} < D_{\min} \quad (14)$$

$$x_{i,j} \in \{0, 1\} \quad \forall (i, j) \in A \quad (15)$$

The formulation QSTPI is a quadratic-constrained binary optimization problem due to (13) and NP-hard (Pedersen et al., 2024). Due to the exponential number of constraints induced by the Steiner cut constraints (12), it is reasonable to use a solver which is specialized in separating these constraints, e.g., SCIP-JACK (Rehfeldt & Koch, 2023). As an extension to the general framework SCIP (Bestuzheva et al., 2023), which can handle mixed integer nonlinear programs (MINLP), one could integrate the quadratic constraint (13) directly. However, preliminary experiments have shown that explicitly linearizing the bilinear products $x_{i,i'} x_{j,j'}$ in (13) appears to be faster. By introducing additionally variables $m_{i,j}$, (13) can be replaced as follows:

$$I_{\text{tot}} \geq \sum_{i \in T_p} \sum_{j \neq i \in T_p} I_{ij} m_{i,j} \quad (16)$$

$$m_{i,j} \geq x_{i,i'} + x_{j,j'} - 1 \quad \forall i < j \in T_p, \quad (17)$$

$$m_{i,j} \geq 0 \quad \forall i < j \in T_p. \quad (18)$$

As the total interference I_{tot} is bounded from above in (12), no upper bound has to be imposed on m .

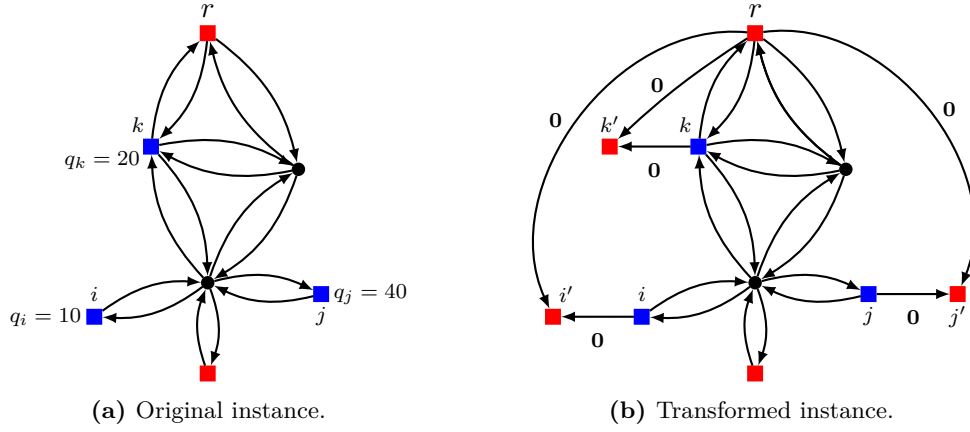


Figure 1: Transformation of QSTPI. For each potential terminal $i \in T_p$ (blue squares) a fixed terminal (red square) i' is added, which is connected to the root node r and the original vertex by an arc of zero costs.

3.4 The flow-based approach

Due to the exponential number of constraints (11), which cannot be handled by general MIP solvers out-of-the-box, the problem can alternatively be modeled by a standard flow-based MIP formulation, commonly used in such applications; see, e.g., Fischetti and Fischetti (2022). The flow-based MIP formulation of the non-transformed QSTPI is given by

$$\min \quad c^T x + b^T y \quad (19)$$

$$\text{s.t.} \quad (20)$$

$$\sum_{v \in T_p} q_v y_v - I_{\text{tot}} \geq Q \quad (21)$$

$$I_{\text{tot}} \geq \sum_{v \in T_p} \sum_{u \neq v \in T_p} I_{uv} y_u y_v \quad (22)$$

$$\sum_{a \in \delta^-(v)} f_a - \sum_{a \in \delta^+(v)} f_a = \begin{cases} 0 & \forall v \in V \setminus (T_f \cup T_p) \\ 1 & \forall v \in T_f \setminus \{r\} \\ y_v & \forall v \in T_p \end{cases} \quad (23)$$

$$x_a \leq y_v \quad \forall a \in \delta^-(v), \forall v \in T_p \quad (24)$$

$$f_a \leq M x_a \quad \forall a \in A \quad (25)$$

$$y_v \in \{0, 1\} \quad \forall v \in T_p \quad (26)$$

$$x_a \in \{0, 1\}, f_a \in \mathbb{R}_{\geq 0} \quad \forall a \in A \quad (27)$$

where x and y denote the decision variables if an arc and a vertex is chosen, respectively, and f describes the flow over the arcs. Constraint (21) describes the quota constraint including the total interference I_{tot} caused by the chosen turbines in (22). The flow balance at each vertex depends on its type and is captured by constraint (23). Any fixed terminal, i.e., the substations, which is not the root, has to be connected to the root node, so a “flow” f of one has to reach the terminal, i.e., the right-hand side is equal to one. Also, any chosen potential terminal (turbine), i.e., $y_v = 1$, has to be connected to the root node. The incoming arcs of a potential terminal can only be active if the potential terminal is chosen, as in (24). Equation (25) ensures that a flow over an arc is only possible if the arc is active. The big-M notation is used to limit the flow on an active arc, i.e., the upper bound on f_a . We choose $M = |T_f \cup T_p|$ as an upper limit, which would allow all fixed and potential terminals to be connected via a single string.

4 Split the problem in two

In this section, we introduce a splitting strategy based on lower bounds on the interference. We will use this method to accelerate the solution process for practical instances of the QSTPI later on.

4.1 Bounding local interference

Concerning wind farms, the layout problem promotes solutions with wide-spread wind turbine positions, whereas the cable routing problem aims to have them as close as possible to the substation. Furthermore, the linearization (17) allows for highly fractional solutions of the LP-relaxation with values $x_i = x_j = 0.5$ and $m_{ij} = 0$, which means that i and j contribute to the quota, but not to the interference value, thus causing highly fractional solutions. Fischetti and Fischetti (2022) present cuts that increase the lower bound of interference caused by choosing to install a turbine, and that have also been useful for hard quadratic problems, see Fischetti et al. (2012). A particular and effective cut is given by

$$I_i \geq \text{LB}_i x_{i,i'}, \quad \forall i \in T_p \tag{28}$$

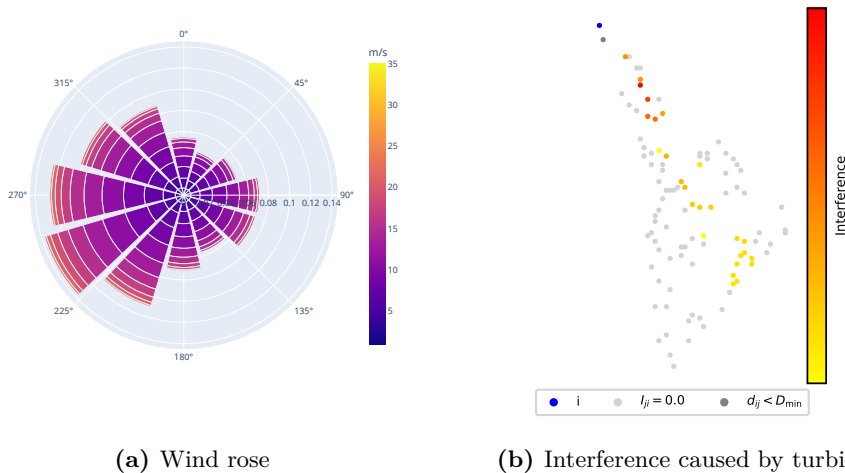


Figure 2: Wind rose of Ten Noorden van de Waddeneilanden site (Panel 2a); Interference caused by turbine i in chosen wind scenario for a sampled instance of wind farm area A (Panel 2b); Interference calculated by the Jensen Model (Jensen, 1983). Wind farm and wind data from Cazzaro and Pisinger, 2022a.

where I_i is the total interference caused by turbine i if built and LB_i is a lower bound on that interference. The authors propose that if one aims to build N_{\max} turbines, then LB_i can be chosen as the sum of the $N_{\max} - 1$ lowest values of I_{ij} . However, these cuts are only effective if $LB_i > 0$. Considering large areas with a high number of potential wind turbine locations from which only a small subset is chosen to be built, this lower bound easily becomes zero, thus making the cut pointless. Such a scenario is shown in Fig. 2b, which shows the caused interference by a turbine under a certain wind distribution (Fig. 2a).

4.2 Splitting the total interference

Nevertheless, in reality, the total interference I_{tot} in a wind farm is unlikely to be zero. Motivated by this fact, we split the QSTPI problem into two subproblems as follows: We define a split value $I_{\text{split}} \in \mathbb{R}_{>0}$ for the total interference. In the first subproblem P_{\geq} , which is called the *upproblem*, this split value is imposed as a lower bound on the total interference, i.e., $I_{\text{tot}} \geq I_{\text{split}}$. In the second subproblem P_{\leq} , the *downproblem*, the split value represents the upper bound on the total interference, i.e., $I_{\text{tot}} \leq I_{\text{split}}$. At first, this might seem counterintuitive, as we consider two possibly computationally challenging problems instead of one. However, as we show in Section 5.4, by carefully choosing I_{split} , this approach is very effective in practice. Furthermore, the following

easy observation holds:

Lemma 4.1. *An optimal solution S_{\geq}^* to the problem P_{\geq} is also optimal to QSTPI if P_{\leq} has no solution \bar{S}_{\leq} with $c(\bar{S}_{\leq}) < c(S_{\geq}^*)$.*

Proof. Given an optimal solution S_{\geq}^* to the problem P_{\geq} and let S^* be the optimal solution to QSTPI. If $c(S^*) < c(S_{\geq}^*)$, then S^* is not feasible for P_{\geq} , but must be feasible for P_{\leq} . \square

4.3 A valid lower bound for the total interference

There are multiple ways to choose the split value I_{split} , e.g., as a fixed parameter or based on some heuristic. Let us consider the following minimization problem:

$$\text{MinI : } \min I_{\text{tot}} \tag{29}$$

$$\text{s.t. } \sum_{i \in T_p} q_i y_i - I_{\text{tot}} \geq Q \tag{30}$$

$$I_{\text{tot}} \geq \sum_{i \in T_p} \sum_{j > i \in T_p} (I_{ij} + I_{ji}) y_j y_i \tag{31}$$

$$y_i + y_j \leq 1 \quad \forall i, j \in T_p, i \neq j, d_{ij} < D_{\min} \tag{32}$$

$$y_i \in \{0, 1\} \quad \forall i \in T_p \tag{33}$$

$$I_{\text{tot}} \in \mathbb{R}_{\geq 0}, \tag{34}$$

i.e., the problem is to choose a subset of potential terminals that minimizes the total interference (29), while fulfilling the desired quota (30) and respecting the minimal distance constraints (32). This problem can be seen as a version of the WFLO. As the total interference is minimized in MinI, there will be no solution for QSTPI with a lower interference than in an optimal solution of MinI.

As splitting into up- and downproblem is pointless when $I_{\text{split}} = 0$, we will now give a necessary and sufficient criterion when MinI has an optimal solution of value zero. Let us consider the undirected graph $G_p = (T_p, E_p)$, where for each pair (i, j) of distinct vertices, there is an edge $(i, j) \in E_p$ if and only if $I_{ij} + I_{ji} > 0$ or $d_{ij} < D_{\min}$. A subset of vertices $S \subseteq T_p$ is called an *independent set* in G_p iff there is no edge in E_p that connects any two vertices in S . A *maximum independent set* (MIS) of graph G is an independent set that maximizes $q(S)$.

Theorem 4.2. *Let Q_{MIS}^* be the quota of an MIS in G_p and I_{tot}^* an optimal solution to MinI. Then*

$$Q \leq Q_{\text{MIS}}^* \Leftrightarrow I_{\text{tot}}^* = 0 \quad (35)$$

Proof. The total interference of MinI is bounded by zero from below. Let S be an MIS and set $y_i := 1$ if and only if $i \in S$. By definition, S does not contain any pair (i, j) of vertices with $I_{ij} + I_{ji} > 0$ or $d_{ij} < D_{\text{min}}$, so that (31) and (32) trivially hold. Moreover, (30) reads as $Q_{\text{MIS}}^* - I_{\text{tot}} \geq Q$. In particular, $I_{\text{tot}} = 0$ is feasible and hence optimal for MinI if and only if $Q_{\text{MIS}}^* \geq Q$. \square

Rephrasing Theorem 4.2, a necessary condition for a non-trivial total interference ($I_{\text{tot}} > 0$) is that $Q > Q_{\text{MIS}}^*$. Combining Lemma 4.1 and Theorem 4.2, we obtain:

Corollary 4.3. *Let I_{LB} be a valid lower bound on the problem MinI. An optimal solution S_{\geq}^* to the problem P_{\geq} is also optimal to P if I_{LB} is chosen as split value I_{split} .*

That means, by finding a valid lower bound to MinI greater than zero, only the smaller upproblem P_{\geq} has to be solved to solve the full QSTPI.

5 Computational Study

In the following, we describe the implementation and the setup of our computational study in Section 5.1 and Section 5.2, respectively. Furthermore, we present the data used in this study in Section 5.3. We conclude this section by demonstrating the strength of our approach compared to the state-of-the-art general MIP solver GUROBI in Section 5.4.

5.1 Implementation

Based on the promising results shown in Pedersen et al. (2024), we have integrated the QSTPI as in Section 3.3 into the Steiner tree software package SCIP-JACK. The exponentially-many constraints (11) are separated using the sophisticated maximum-flow algorithm implemented by Rehfeldt (2021) which is based on the classical max-flow/min-cut theorem. Additionally to the separation procedure, the solution process is supported by a *shortest-path heuristic* (SPH).

In general, heuristics are utilized to find good and feasible solutions in short time to provide upper bounds on the exact solution of the problem. Within the context of STP-related problems, the SPH is the best-known heuristic and was introduced by Takahashi and Matsuyama (1980). For this study, we adapt SCIP-JACK’s SPH implementation by Rehfeldt (2021) and already customized for the case of the QSTP by Pedersen et al. (2024): Starting at the root r , the closest fixed terminal or potential terminal is inserted to the *root component*. The interference between the newly inserted node and all nodes in the root component is calculated and added to the total interference. Then, the distance of all non-connected vertices to the root component is updated. This process is repeated until all fixed terminals are connected and the connected potential terminals minus the total interference fulfill the desired quota. Preliminary experiments have shown that, although the SPH finds good upper bounds at the root node, it rarely improves the primal bound during the branch-and-bound procedure. Therefore, we decided to run the SPH only at the root node, modifying the arc costs to $\bar{c}_a := (1.0 - \hat{x}_a)c_a$ for all $a \in A$ depending on the current LP-solution \hat{x} .

Our solver will be benchmarked against a black-box MIP solver using the flow-based formulation presented in Section 3.4.

5.2 Computational setting

The QSTPI is integrated into SCIP-JACK using SCIP 8.0.1 (Bestuzheva et al., 2023) with CPLEX 12.10 (IBM ILOG, 2022) as LP solver. The flow-based MIP formulation is implemented using the GUROBI PYTHON-interface in PYTHON 3.11.2, and is solved with GUROBI 11.01 (Gurobi Optimization, LLC, 2024). The following settings are run:

- FLOW: the basic flow-based model, presented in (19) - (27);
- FLOW-S-0.1: as before, but using the up- and downproblem approach, described in Section 4, with $I_{\text{split}} := 0.1$;
- QSTPI: the QSTPI formulation presented in (10) - (18);
- QSTPI-S-0.1: as before, but using the up- and downproblem approach, described in Section 4, with $I_{\text{split}} := 0.1$;

- QSTPI-S-H α : as before, but I_{split} is determined using the interference value from the initial shortest-path heuristic solution multiplied by $\alpha \in \{0.1, 0.5, 0.8\}$;
- QSTPI-S-minI- τ : as before, but $I_{\text{split}} := \max(0.1, I_{\text{tot}}^*)$, where I_{tot}^* corresponds to the best primal solution of the minimization problem MinI presented in (29) - (34) within a time limit of $\tau \in \{300, 600, 1800\}$ seconds using SCIP 8.0.1.

All computational experiments are executed single-threaded in a non-exclusive mode on a cluster with *Intel(R) Xeon(R) Gold 6338* CPUs running at 2.00 GHz, where four CPUs and 64 GB of RAM are reserved for each run. For a better comparison with our implementation in SCIP-JACK, which is only single-threaded, we restrict the black-box solver GUROBI to one thread when discussing the results. However, further experiments have shown that under the given setup no performance improvement is gained when running GUROBI in 8-threaded mode. We set a time limit of six hours (21,600 s). The downproblem is only solved if the upproblem is solved to optimality. In this case, the downproblem is run using the optimal objective value of the upproblem as an objective bound (see Lemma 4.1).

5.3 Data creation

As a benchmark set, we use three representative wind farm instances out of the dataset introduced by Cazzaro and Pisinger (2022a), namely instances A, B, and C. Instance A and C are divided into two zones of which we only consider the larger zone; see Fig. 3. For each wind farm, we create 20 small-, medium-, and large-sized instances each by randomly sampling 100, 200, and 500 potential positions, respectively.

For instance A we set the quota equivalent to the power production of 10 and 20 wind turbines for all sampled instances. For instance B the quota is set to 10, 20, and 40 wind turbines for the small-sized instances and 10, 20, 40, and 60 for the medium- and large-sized instances. For instance C the quota of the small-sized instances is set to 10 and 20, for the medium-sized to 10, 20, and 40, and for the large-sized ones to 10, 20, 40, and 60 wind turbines. Due to unlucky sampling, too many turbines might be too close to each other to satisfy the quota constraint. Removing these trivially infeasible instances, our complete benchmark set has 143 small-, 180 medium-, and 200 large-sized instances.

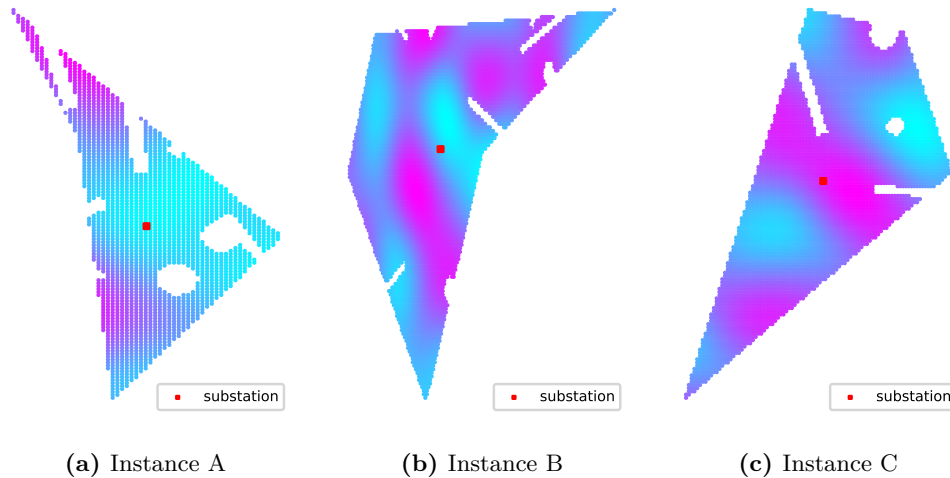


Figure 3: Chosen representative wind farms by Cazzaro and Pisinger, 2022a. Color of regions represents the costs of building a turbine from low to high costs.

The interference is calculated by the Jensen model (Jensen, 1983) based on real wind measurements at Ten Noorden van de Waddeneiladen² given in the dataset by Cazzaro and Pisinger (2022a); see Fig. 2a. Fig. 2b shows the interference caused by a turbine under the considered wind scenario in an exemplary sample of instance A. No information regarding the position of the substation is given in the original dataset. Therefore, the substation is placed in the middle of each area, i.e., the coordinates of the substation are given by averaging the coordinates of all available positions. The cost to build a turbine at a specific position is also given in the dataset by Cazzaro and Pisinger (2022a) and represents the foundation costs. We use the 15 MW turbines with a rotor diameter of 240 meters in the dataset by Cazzaro and Pisinger (2022a). The minimum distance required between two turbines is usually three to five times the rotor diameter; we set the minimum distance D_{\min} to 1200 meters. The cable costs are chosen in accordance to Cazzaro et al. (2020). The authors provide cable costs for three types of cables: 430, 480, and 610 k€/km. Since we do not consider cable capacities in this study, a mean value of 504 k€/km is chosen.

5.4 Results

Fig. 4 shows the cumulative percentage of instances solved to optimality over time for the complete problem (left) and for the upproblem (right) for all settings. Note, that

²reported by <https://offshorewind.rvo.nl/>

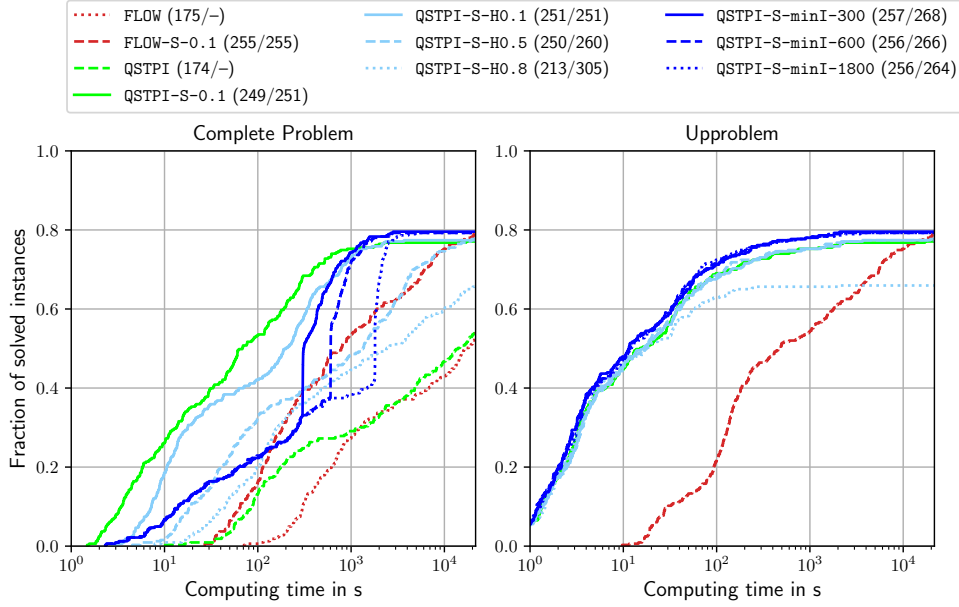


Figure 4: Performance profiles for small- and medium-sized instances. Left: Cumulative percentage of instances solved to optimality over time for all settings. Right: Cumulative percentage of instances solved by the upproblem for which also the downproblem is solved over time spend on the upproblem. The numbers in brackets state the number of instances which are solved to optimality completely and instances for which the upproblem is solved to optimality.

only instances that are solved to optimality for the complete problem are shown in the right plot. In the legend of the figure, the first number in the brackets reports the number of instances completely solved to optimality. The second number gives the number of instances, for which the upproblem was solved to optimality.

Whereas the simple QSTP without the interference and minimum distance constraints has outperformed the flow-based formulation by up-to two orders of magnitude before (see Pedersen et al. (2024)), this advantage vanishes complete considering QSTPI and FLOW. Both settings only manage to solve 174 and 175 out of 323 instances in the time limit of six hours, respectively. By introducing a split value of $I_{\text{split}} = 0.1$, the performance increases drastically. FLOW-S-0.1 is not only a magnitude faster than QSTPI and FLOW, but also solves 81 and 80 more instances, respectively. Applying the same split value on our approach in QSTPI-S-0.1, the performance is increased by another magnitude solving 249 of 323 instances to optimality. Remarkably, all these instances are solved within roughly one hour: In relation to that, GUROBI only solves less than 70% of the instances in that time.

Considering QSTPI-S-H α , the best performance is achieved with $\alpha = 0.1$, be-

ing around a magnitude faster than $\alpha = 0.5$ and $\alpha = 0.8$. `QSTPI-S-H0.1` and `QSTPI-S-H0.5` solve 251 out of 323 instances to optimality, whereas `QSTPI-S-H0.8` only solves 213 instances. By using a higher split value the better is the performance in solving the number of instance for the upproblem, i.e., 251, 260, and 305 for α equal to 0.1, 0.5, and 0.8, respectively (see the second number in the brackets in the legend of Fig. 4). However, the downproblem becomes much harder to solve, and 0, 10, and 88 instances run into the time limit in the downproblem for α equal 0.1, 0.5, and 0.8, respectively.

For the settings `QSTPI-S-minI- τ` the majority of instances run into the time limit of τ in the starting problem (200 for τ equal 300s and 600s, and 177 for τ equal 1800s). This also explains the sudden increase in solved instances around that time, as using the solution of the starting problem results in solving the integrated problem very fast for some instances. `QSTPI-S-minI-300` solves 257 out of 323 instances to optimality, the other two solve 256. For 108 instances the proven optimality for minimal interference is zero considering the starting problem, i.e., the default value 0.1 is used as a split value. For 214 instances, all the three settings give a split value higher than the default value of 0.1. For τ equal 300s, 600s, and 1800s, the starting problem gives a lower bound greater zero for the starting problem for 168, 191, and 202 instances, respectively, which can be used for the downproblem, and thus, speeding up its solving process. Out of these instances, for 13, 13, and 31 the split value is the optimal solution of the starting problem, and hence, provides a valid lower bound on the interference in the upproblem and the downproblem has not to be solved at all. Taking a look at the performance with respect to the upproblem on the right of Fig. 4 shows that all settings using the extended QSTP formulation perform similarly and much better than using the out-of-the-box solver `GUROBI`, except for `QSTPI-S-H0.8` which solves 42 less instances to optimality. Regarding the instances that are not solved to optimality, these are, in particular, the medium sized instances with a high quota.

The performance profiles in Fig. 4 have already shown the advantages of our novel approach for the IWFLCR problem. In the following, the setting `QSTPI-S-0.1` is first compared instance-wise to `FLOW` and then to `FLOW-S-0.1` in Fig. 5 and Fig. 6. For the pairwise comparison we only consider instances solved to optimality by both settings. In the legend, additional to the arithmetic mean of the speedup, the shifted geometric

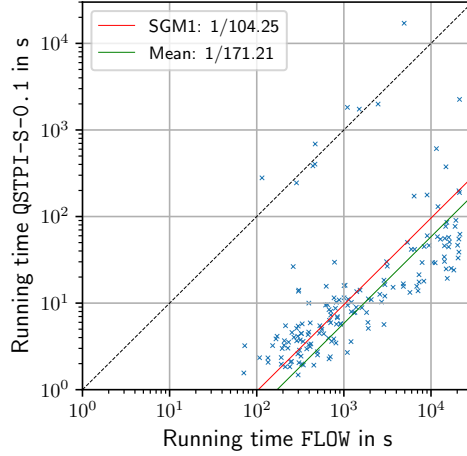


Figure 5: Comparison of running times between QSTPI-S-0.1 and FLOW of all instances solved by both settings.

mean with a shift of 1 (SGM1) is reported. The *shifted geometric mean* (Achterberg, 2007) has become a standard measure in discrete optimization (Mittelmann, 2020) and is less biased towards harder instances. By using QSTPI-S-0.1 instead of FLOW an average speedup of 171.21 and a SGM1 of 104.25 is achieved, where QSTPI-S-0.1 is faster on all but 5 instances, see Fig. 5. For the complete problem, QSTPI-S-0.1 is 30.98 times faster on average and 14.90 times faster considering the SGM1 compared to FLOW-S-0.1 ; see 6a. These factors increase by around two if only the upproblem is considered, i.e., 59.36 and 34.36 for the arithmetic mean and the SGM1, respectively, see Fig. 6b.

The benefit of our novel approach becomes even more prominent when we are looking at the performance for the large-sized instances in Fig. 7. For these instances, the basic settings FLOW and QSTPI cannot solve any instance to optimality. The setting FLOW-S-0.1 only solves 7 instances out of 200 to optimality and 40 in the upproblem. The best setting is QSTPI-S-0.1 solving 64 out of 200 instances to optimality and 106 instances in the upproblem. Considering the settings $\text{QSTPI-S-H}\alpha$, again the smaller the α the better is the performance for the complete problem. However, only maximal 22 instances can be solved to optimality using these settings. For $\text{QSTPI-S-minI-}\tau$, we ignore $\tau = 300$, as SCIP cannot find any primal solution for the starting problem within the time limit of 300 seconds. The performance of QSTPI-S-minI-600 and QSTPI-S-minI-1800 is the same solving 38 instances to optimality.

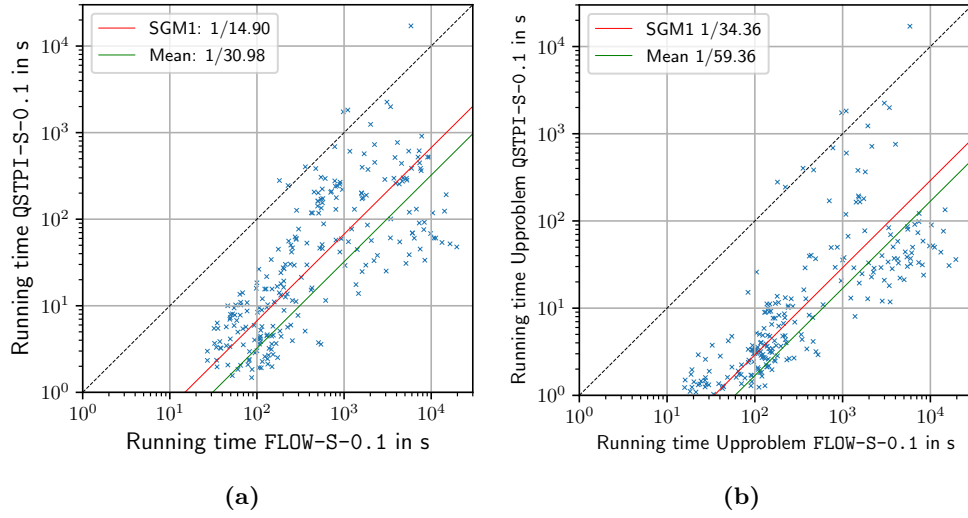


Figure 6: Comparison of total running times (Panel 6a) and running times of the upproblem (Panel 6b) between QSTPI-S-0.1 and FLOW-S-0.1 of all instances solved by both settings.

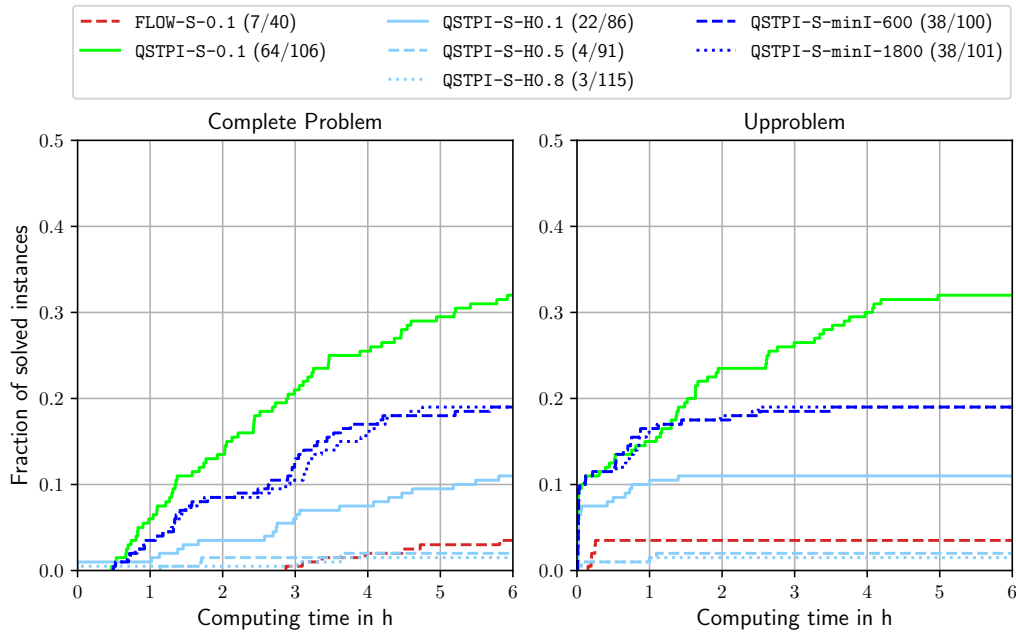


Figure 7: Performance profiles for large-sized instances. Left: Cumulative percentage of instances solved to optimality over time for all settings. Right: Cumulative percentage of instances solved by the upproblem for which also the downproblem is solved over time spent on the upproblem. The numbers in brackets state the number of instances which are solved to optimality completely and instances for which the upproblem is solved to optimality. Note: The y-axis is limited to 0.5.

6 Price of sequentiality

The common approach of solving the wind farm layout and cable routing problem sequentially can lead to suboptimal solutions. As a final evaluation, we illustrate the price of that sequentiality. We compare our integrated approach with the sequential equivalent, which consists of first finding a feasible positioning minimizing the turbine costs, followed by computing the minimum spanning tree of the complete subgraph containing these turbines and the substation. The minimization problem in the first step is formulated as:

$$\min \sum_{i \in T_p} b_i y_i \quad (36)$$

$$\text{s.t. } (30) - (34), \quad (37)$$

and is solved with GUROBI 11.01. The minimum spanning tree is computed using Kruskal’s algorithm provided by the PYTHON-package NETWORKX (Hagberg et al., 2008). The test set consists of the 257 small- and medium-sized instances solved to optimality by the setting QSTPI-S-minI-300. The relative cost reduction is calculated by

$$c_{\text{rel.}}^{\text{red}} = \left(1 - \frac{c_{\text{integrated}}}{c_{\text{sequential}}} \right) \cdot 100\%.$$

Fig. 8 presents the relative cost reduction of the integrated approach in comparison to the sequential approach for each instance, showing a mean reduction of 8.39% with a maximal reduction of 33.5%. Fig. 9 shows an exemplary solution for instance B for the scenario of 20 turbines and a 8% reduction in costs by using the integrated approach. We conclude that the price of sequentiality is significant and justifies invoking an integrated approach.

7 Conclusion and outlook

Current methods for solving the integrated wind farm layout and cable routing problem (IWFLCR) are either heuristic approaches or are limited to very small instances. This paper proposes a new approach for optimizing simultaneously the turbine locations

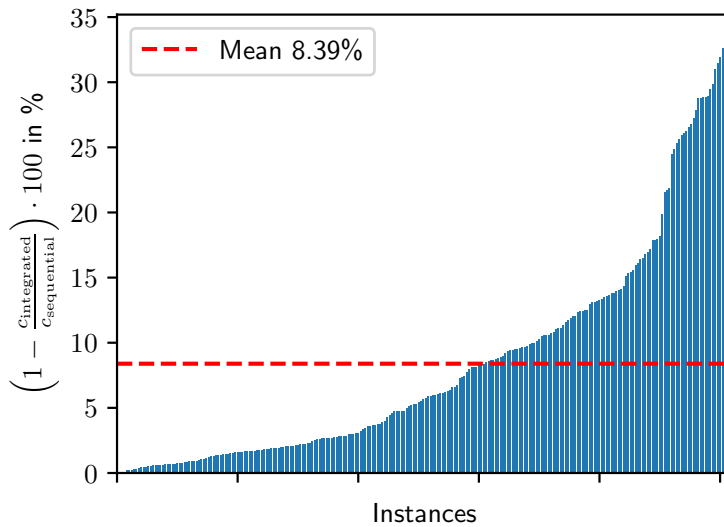
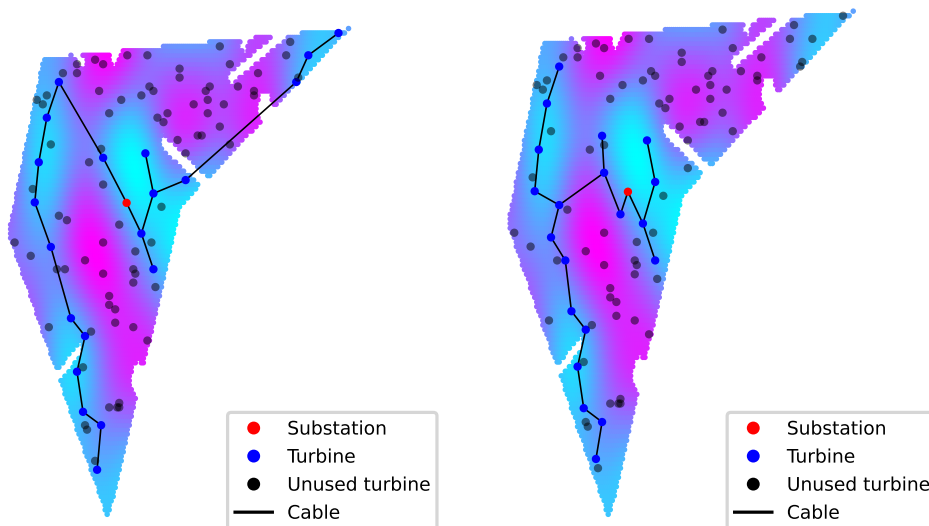


Figure 8: Cost reduction by using the integrated approach compared to the sequential approach for all instances which are solved to optimality.



(a) Solution for the sequential approach (b) Solution for the integrated approach

Figure 9: Exemplary comparison of sequential vs. integrated approach: The integrated method achieves a total cost reduction of 8% compared to the sequential one.

and their connection to the grid’s substation. The core is the QSTPI, an extension of the Quota Steiner tree problem (QSTP). Besides the quota and connectivity constraints from the QSTP, the formulation includes the wake effect caused by a turbine reducing the profit of the surrounding turbines, and complies with the minimal distance required between chosen turbines. Both are vital technical constraints for the

WFLO. We have upgraded the state-of-the-art STP-solver SCIP-JACK so that it can handle the interference-constrained variant of the QSTP. Where the basic QSTP is of great advantage compared to standard flow-based formulation solvable by general MIP solvers, its interference-constrained variant bears no advantage at first. On the one hand this shows the immense difficulty of the quadratic constraints induced by the wake effect, and on the other hand the great improvements made by generic MIP solvers for these types of constraints.

Inspired by known cutting planes for the interference constraint, we therefore propose a solution strategy of splitting the problem based on the total interference. Although two possibly challenging subproblems must be solved, we demonstrate on a large testset that a) the solution strategy speedups the solution process and makes most of the instances solvable, and b) the advanced version of SCIP-JACK outperforms standard MIP solvers and is capable of finding optimal solutions for large-sized instances, where general state-of-the-art MIP solvers struggle. In particular, using a relatively small fixed value of 0.1 for splitting the interference region (see results for QSTPI-S-0.1) has been proven fruitful on our dataset. Finally, we illustrate that to avoid excessive design costs for wind farm projects, an integrated view of the WFLO and WFCR is beneficial.

Although our presented extensions to SCIP-JACK outperforms general MIP solvers in terms of computational time as well as in solving large-sized instances, there are several instances of the considered dataset that have not been solved to optimality. As stated in Section 5.1, the chosen primal heuristic often improves the primal solution only at the root node of the branch-and-bound tree, more efficient and suitable primal heuristics should be investigated.

Furthermore, improving the dual bound of the presented formulation is vital. However, the cuts proposed by Fischetti and Fischetti (2022) introduce very dense rows in the constraint matrix, making the LP-relaxation harder to solve, and preliminary experiments show that while improving the root node relaxation, the overall performance worsens.

In this study, the IWFLCR problem is approached by a variant of the STP, so that the solution is also a Steiner tree. To make the approach even more applicable to the actual design process of the wind farm, cable capacities should be considered; see, e.g.,

Cazzaro and Pisinger (2022b). In the context of STP, some complexity results for the edge capacitated STP variant are given in Bentz et al. (2020).

Acknowledgements

The work for this article has been conducted in the Research Campus MODAL funded by the German Federal Ministry of Education and Research (BMBF) (fund numbers 05M14ZAM, 05M20ZBM), and the project “Stadt-Land-Energie – Robustheit und Übertragbarkeit von interkommunalen Energiewendeszenarien im Stadt-Land-Nexus” (Stadt-Land-Energie) funded by Forschungszentrum Jülich GmbH with funds of the Ministry for Economic Affairs and Climate Action (BMWK) (fund number 03EI1051A-B). We thank Davide Cazzaro for making his code available to compute the interference matrix for the used dataset.

CRedit statement

Conceptualization: J.P., T.K.; data curation: J.P.; formal analysis: J.P., N.L.; investigation: J.P.; methodology: J.P., N.L., D.R.; software: J.P., D.R.; validation: J.P.; visualization: J.P.; writing – original draft: J.P.; writing – review and editing: J.P., N.L., D.R.

References

- Achterberg, T. (2007). *Constraint integer programming* [Doctoral dissertation, Technische Universität Berlin]. <https://opus4.kobv.de/opus4-zib/frontdoor/index/index/docId/1018> (Accessed on 12/04/2024).
- Archer, R., Nates, G., Donovan, S., & Waterer, H. (2011). Wind turbine interference in a wind farm layout optimization mixed integer linear programming model. *Wind Engineering*, 35(2), 165–175. <https://doi.org/10.1260/0309-524X.35.2.165>
- Bentz, C., Costa, M.-C., & Hertz, A. (2020). On the edge capacitated steiner tree problem. *Discrete Optimization*, 38, 100607. <https://doi.org/https://doi.org/10.1016/j.disopt.2020.100607>
- Bestuzheva, K., Besançon, M., Chen, W.-K., Chmiela, A., Donkiewicz, T., van Doornmalen, J., Eifler, L., Gaul, O., Gamrath, G., Gleixner, A., Gottwald, L., Graczyk, C., Halbig, K., Hoen, A., Hojny, C., van der Hulst, R., Koch, T., Lübbecke, M., Maher, S. J., ... Witzig, J. (2023). Enabling Research through the SCIP Optimization Suite 8.0. *ACM Transactions on Mathematical Software*. <https://doi.org/10.1145/3585516>
- Bolukbasi, G., & Kocaman, A. S. (2018). A prize collecting Steiner tree approach to least cost evaluation of grid and off-grid electrification systems. *Energy*, 160, 536–543. <https://doi.org/10.1016/j.energy.2018.07.029>
- Cazzaro, D., & Pisinger, D. (2022a). Variable neighborhood search for large offshore wind farm layout optimization. *Computers & Operations Research*, 138. <https://doi.org/10.1016/j.cor.2021.105588>
- Cazzaro, D., Fischetti, M., & Fischetti, M. (2020). Heuristic algorithms for the wind farm cable routing problem. *Applied Energy*, 278, 115617. <https://doi.org/10.1016/j.apenergy.2020.115617>
- Cazzaro, D., Koza, D. F., & Pisinger, D. (2023). Combined layout and cable optimization of offshore wind farms. *European Journal of Operational Research*, 311(1), 301–315. <https://doi.org/10.1016/j.ejor.2023.04.046>

- Cazzaro, D., & Pisinger, D. (2022b). Balanced cable routing for offshore wind farms with obstacles. *Networks*, *80*(4), 386–406. <https://doi.org/https://doi.org/10.1002/net.22100>
- Donovan, S. (2005). Wind farm optimization. *Proceedings of the 40th annual ORSNZ conference*, 196–205.
- Fischetti, M. (2021). On the optimized design of next-generation wind farms. *European Journal of Operational Research*, *291*(3), 862–870. <https://doi.org/10.1016/j.ejor.2020.10.048>
- Fischetti, M., & Pisinger, D. (2018). Optimizing wind farm cable routing considering power losses. *European Journal of Operational Research*, *270*(3), 917–930. <https://doi.org/10.1016/j.ejor.2017.07.061>
- Fischetti, M., & Fischetti, M. (2022). Integrated Layout and Cable Routing in Wind Farm Optimal Design. *Management Science*. <https://doi.org/10.1287/mnsc.2022.4470>
- Fischetti, M., & Monaci, M. (2016). Proximity search heuristics for wind farm optimal layout. *Journal of Heuristics*, *22*, 459–474.
- Fischetti, M., & Pisinger, D. (2019). Mathematical optimization and algorithms for offshore wind farm design: An overview. *Business & Information Systems Engineering*, *61*, 469–485.
- Fischetti, M., Monaci, M., & Salvagnin, D. (2012). Three ideas for the quadratic assignment problem. *Operations research*, *60*(4), 954–964.
- González, J. S., Payán, M. B., Santos, J. M. R., & González-Longatt, F. (2014). A review and recent developments in the optimal wind-turbine micro-siting problem. *Renewable and Sustainable Energy Reviews*, *30*, 133–144. <https://doi.org/https://doi.org/10.1016/j.rser.2013.09.027>
- Gurobi Optimization, LLC. (2024). Gurobi Optimizer Reference Manual, Version 11.0.1. <https://www.gurobi.com>.
- Hagberg, A. A., Schult, D. A., & Swart, P. J. (2008). Exploring network structure, dynamics, and function using networkx. In G. Varoquaux, T. Vaught, & J. Millman (Eds.), *Proceedings of the 7th python in science conference* (pp. 11–15).
- Hou, P., Zhu, J., Ma, K., Yang, G., Hu, W., & Chen, Z. (2019). A review of offshore wind farm layout optimization and electrical system design methods. *Journal of Modern Power Systems and Clean Energy*, *7*(5), 975–986.
- IBM ILOG. (2022). V12.10: User’s Manual for CPLEX. <https://www.ibm.com/analytics/cplex-optimizer>.
- Jansen, M., Staffell, I., Kitzing, L., Quoilin, S., Wiggelinkhuizen, E., Bulder, B., Riepin, I., & Müsgens, F. (2020). Offshore wind competitiveness in mature markets without subsidy. *Nature Energy*, *5*(8), 614–622. <https://doi.org/10.1038/s41560-020-0661-2>
- Jensen, N. (1983). *A note on wind generator interaction*. Risø National Laboratory.
- Johnson, D. S., Minkoff, M., & Phillips, S. (2000). The prize collecting Steiner tree problem: Theory and practice. *Proceedings of the Eleventh Annual ACM-SIAM Symposium on Discrete Algorithms*, 760–769.
- Karp, R. M. (1972). Reducibility among Combinatorial Problems. In R. E. Miller, J. W. Thatcher, & J. D. Bohlinger (Eds.), *Complexity of Computer Computations: Proceedings of a symposium on the Complexity of Computer Computations, held March 20–22, 1972, at the IBM Thomas J. Watson Research Center, Yorktown Heights, New York, and sponsored by the Office of Naval Research, Mathematics Program, IBM World Trade Corporation, and the IBM Research Mathematical Sciences Department* (pp. 85–103). Springer US. https://doi.org/10.1007/978-1-4684-2001-2_9
- Klimm, F., Toledo, E. M., Monfeuga, T., Zhang, F., Deane, C. M., & Reinert, G. (2020). Functional module detection through integration of single-cell RNA sequencing data with protein–protein interaction networks. *BMC Genomics*, *21*(1), 756. <https://doi.org/10.1186/s12864-020-07144-2>
- Koch, T., Berthold, T., Pedersen, J., & Vanaret, C. (2022). Progress in mathematical programming solvers from 2001 to 2020. *EURO Journal on Computational Optimization*, *10*, 100031. <https://doi.org/https://doi.org/10.1016/j.ejco.2022.100031>

- Leitner, M., Ljubic, I., Luipersbeck, M., Prosegger, M., & Resch, M. (2014, January). *New Real-world Instances for the Steiner Tree Problem in Graphs* (tech. rep.).
- Ljubić, I. (2021). Solving Steiner trees: Recent advances, challenges, and perspectives. *Networks*, *77*(2), 177–204. <https://doi.org/10.1002/net.22005>
 _eprint: <https://onlinelibrary.wiley.com/doi/pdf/10.1002/net.22005>.
- Ljubić, I., Weiskircher, R., Pferschy, U., Klau, G. W., Mutzel, P., & Fischetti, M. (2006). An Algorithmic Framework for the Exact Solution of the Prize-Collecting Steiner Tree Problem. *Mathematical Programming*, *105*(2), 427–449. <https://doi.org/10.1007/s10107-005-0660-x>
- Mittelman, H. (2020). Benchmarks for optimization software. <http://plato.asu.edu/bench.html>.
- Our World in Data. (2021). Installed wind energy capacity. <https://ourworldindata.org/grapher/cumulative-installed-wind-energy-capacity-gigawatts> (Accessed on 08/21/2021).
- Pedersen, J., & Ljubić, I. (2025). Prize-collecting steiner tree problem and its variants. In P. M. Pardalos & O. A. Prokopyev (Eds.), *Encyclopedia of optimization* (pp. 1–11). Springer International Publishing. https://doi.org/10.1007/978-3-030-54621-2_869-1
- Pedersen, J., Weinand, J. M., Syranidou, C., & Rehfeldt, D. (2024). An efficient solver for large-scale onshore wind farm siting including cable routing. *European Journal of Operational Research*, *317*(2), 616–630. <https://doi.org/10.1016/j.ejor.2024.04.026>
- Pryor, S. C., Barthelmie, R. J., Bukovsky, M. S., Leung, L. R., & Sakaguchi, K. (2020). Climate change impacts on wind power generation. *Nature Reviews Earth & Environment*, *1*(12), 627–643. <https://doi.org/10.1038/s43017-020-0101-7>
- Pryor, S. C., Barthelmie, R. J., & Shepherd, T. J. (2021). Wind power production from very large offshore wind farms. *Joule*, *5*(10), 2663–2686.
- Rehfeldt, D. (2021). *Faster algorithms for Steiner tree and related problems: From theory to practice* [Doctoral dissertation, Technische Universität Berlin]. <https://opus4.kobv.de/opus4-zib/frontdoor/index/index/docId/8514> (Accessed on 02/24/2023).
- Rehfeldt, D., & Koch, T. (2022). On the Exact Solution of Prize-Collecting Steiner Tree Problems. *INFORMS Journal on Computing*, *34*(2), 872–889. <https://doi.org/10.1287/ijoc.2021.1087>
- Rehfeldt, D., & Koch, T. (2023). Implications, conflicts, and reductions for steiner trees. *Mathematical Programming*, *197*, 903–966. <https://doi.org/10.1007/s10107-021-01757-5>
- Rehfeldt, D., Koch, T., & Maher, S. J. (2019). Reduction techniques for the prize collecting Steiner tree problem and the maximum-weight connected subgraph problem. *Networks*, *73*(2), 206–233. <https://doi.org/10.1002/net.21857>
- Ridremont, T. (2019, April). *Design of robust networks. Application to the design of wind farm cabling networks*. [Doctoral dissertation, Polytechnique Montréal]. <https://publications.polymtl.ca/3889/> (Accessed on 03/02/2023).
- Samorani, M. (2013). The wind farm layout optimization problem. In P. M. Pardalos, S. Rebennack, M. V. F. Pereira, N. A. Iliadis, & V. Pappu (Eds.), *Handbook of wind power systems* (pp. 21–38). Springer Berlin Heidelberg. https://doi.org/10.1007/978-3-642-41080-2_2
- Takahashi, H., & Matsuyama, A. (1980). An approximate solution for the Steiner problem in graphs. *Mathematica Japonica*, *(6)*, 573–577.
- Turner, S., Romero, D., Zhang, P., Amon, C., & Chan, T. (2014). A new mathematical programming approach to optimize wind farm layouts. *Renewable Energy*, *63*, 674–680.
- Veers, P., Dykes, K., Lantz, E., Barth, S., Bottasso, C. L., Carlson, O., Clifton, A., Green, J., Green, P., Holttinen, H., Laird, D., Lehtomäki, V., Lundquist, J. K., Manwell, J., Marquis, M., Meneveau, C., Moriarty, P., Munduate, X., Muskulus, M., . . . Wiser, R. (2019). Grand challenges in the science of wind energy. *Science (New York, N.Y.)*, *366*(6464). <https://doi.org/10.1126/science.aau2027>
- Wiser, R., Jenni, K., Seel, J., Baker, E., Hand, M., Lantz, E., & Smith, A. (2016). Expert elicitation survey on future wind energy costs. *Nature Energy*, *1*(10). <https://doi.org/10.1038/nenergy.2016.135>

- Wiser, R., Rand, J., Seel, J., Beiter, P., Baker, E., Lantz, E., & Gilman, P. (2021). Expert elicitation survey predicts 37% to 49% declines in wind energy costs by 2050. *Nature Energy*, 6(5), 555–565. <https://doi.org/10.1038/s41560-021-00810-z>
- Wong, R. T. (1984). A dual ascent approach for steiner tree problems on a directed graph. *Mathematical Programming*, 28(3), 271–287. <https://doi.org/10.1007/BF02612335>